Elimination of Intergranular Corrosion Susceptibility of Cold-Worked and Sensitized AISI 316 SS by Laser Surface Melting

N. Parvathavarthini, R.V. Subbarao, Sanjay Kumar, R.K. Dayal, and H.S. Khatak

(Submitted 26 March 2000)

Susceptibility to intergranular corrosion (IGC) and intergranular stress corrosion cracking (IGSCC) due to sensitization is one of the major problems associated with austenitic stainless steels. Thermal exposures encountered during fabrication (welding, hot working, *etc.*) and elevated temperature service may lead to sensitization of components of austenitic stainless steels. Laser surface melting (LSM) is an *in-situ* method to increase the life of a sensitized component by modifying the surface microstructure without affecting the bulk properties. In this paper, the results obtained in the attempt to improve IGC resistance of cold-worked and sensitized 316 SS by LSM are presented. Type 316 SS specimens cold worked to various degrees ranging from 5 to 25% reduction in thickness and sensitized to different degrees by exposing at 898 K for different durations were laser surface melted using continuous wave (cw) CO_2 laser. ASTM standard A262 practice A, optical metallography, and ASTM standard G108 were used to characterize the specimens before and after LSM. Influence of prior deformation on the desensitization behavior was evaluated for the laser melting conditions adopted during the investigation. Complete dissolution of $M_{23}C_6$ due to laser melting and suppression of re-precipitation due to rapid quenching result in a desensitized homogenous microstructure, which is immune to IGC. Under identical laser melting conditions, the extent of desensitization decreases with an increase in the degree of cold work, and hence, higher power levels and an extended interaction time must be adopted to homogenize the sensitized microstructure with prior cold work.

Keywords IGSCC, intergranular stress corrosion cracks, laser surface modifications, type 316 stainless steel

1. Introduction

Intergranular corrosion (IGC) and intergranular stress corrosion cracking (IGSCC) are common modes of failure in austenitic stainless steels that have been subjected to elevated temperature treatments and subsequent exposure to corrosive environment. Numerous failures, which have been reported in nuclear and petrochemical industries, have been attributed to IGC and IGSCC.[1,2,3] When austenitic stainless steels are extensively heated or slowly cooled through the temperature regime of 773 to 1073 K, either during fabrication or during service, chromium-rich $M_{23}C_6$ carbides are formed along the grain boundaries. This leads to significant depletion of chromium adjacent to these carbides. Chromium carbide precipitation and the concomitant chromium depletion are referred to as "sensitization." When such a sensitized component is exposed to corrosive solution, IGC or IGSCC occurs, and hence, in order to avoid these forms of attack, sensitized microstructure should be eliminated.

N. Parvathavarthini, R.V. Subbarao, R.K. Dayal, and **H.S. Khatak,** Corrosion Science & Technology Division, Indira Gandhi Centre For Atomic Research, Kalpakkam-603102, Tamilnadu, India; and **Sanjay Kumar,** Regional Institute of Technology, Jamshedpur, India. Contact e-mail: rkd@igar.ernet.in.

Because the mechanism of sensitization has been well understood, several methods have been developed to avoid it. These methods are listed briefly below.

- By employing high-temperature solutionizing and rapid cooling through the sensitization range, sensitization can be avoided. However, such a bulk treatment is not always possible for fabricated components and also large thermal stresses may be introduced into the components due to such rapid quenching.
- By using low-carbon varieties, sensitization can be delayed and weld decay can be avoided. But reduction in carbon leads to lower mechanical strength. Although this can be compensated for by the addition of nitrogen to the low-carbon varieties to produce Low carbon Nitrogen added (LN) stainless steels, prolonged thermal aging of nitrogen-added stainless steel also results in sensitization.
- By alloying with elements that have a greater tendency than chromium to form carbides (Ti and Nb in 321 and 347 SS), stable carbides are formed and sensitization can be avoided. However, welding and the subsequent stress relieving treatment make these carbides more prone to knife line attack.

In the recent past, rapid induction heating was also attempted, by which acceptable recovery of the properties of sensitized material can be achieved. However, if a component is found to be sensitized at the final stage of fabrication or during commissioning or during service, it becomes prone to IGC/IGSCC. The conventional remedies listed above are

impracticable for many components in the nuclear and chemical industries. In such cases, an *in-situ* method is required to selectively eliminate sensitized microstructure at critical locations. Laser surface melting is one among the methods to eliminate sensitization. By the proper choice of laser parameters, a sensitized microstructure can be modified *in situ*, even in high radiation fields and in components with complicated geometry. Several investigations have been carried out to improve the IGC resistance of sensitized 304 SS and 316 SS using high power Nd:YAG laser and cw CO_2 laser under different laser irradiation conditions.[4–18] It has been reported that the laser-melted surface is highly resistant to IGSCC and, hence, is far superior to laser cladding methods for pipes.[4] Nakao and Nishimoto[13] have desensitized the HAZ of the 304 SS surface and have established a time-temperature-desensitization diagram based on the assumption of Cr diffusion control for desensitization phenomena. Jeng *et al.* have reported that the surface melting of type 347 SS using a 2 kW cw CO_2 laser improved resistance against end grain attack in HNO_3 media.[17] The same technique was applied to 304L plates also to eliminate sensitization. Similar results were obtained for type 321 SS by Zamfer *et al.*[18]

Although several studies have been made on a variety of stainless steels, information available on the influence of prior cold work (CW) on the desensitization behavior by LSM is scanty and no systematic study has been reported so far. For several applications of stainless steel, cold working is the final manufacturing operation. Cold work affects the kinetics of sensitization. 316 SS and 316 LN SS are the major structural materials in fast breeder reactors. Cold working is intentionally introduced in core components of fast reactors to improve the swelling resistance under irradiation. Higher degrees of cold work affect some of the mechanical properties such as toughness, creep rupture, low-cycle fatigue, and corrosion resistance. Hence, for nuclear applications, an upper limit of 25% cold work is generally recommended. The present study has been undertaken to investigate the influence of prior cold work on the extent of desensitization behavior of cold-worked and sensitized 316 SS containing nitrogen.

2. Experimental

2.1 Material

The material used in this investigation is AISI type 316 SS in the mill-annealed condition. The chemical composition is given in Table 1.

2.2 Cold Working

The as-received material in the mill-annealed condition was taken as the reference corresponding to a cold work of 0%. Mill-annealed sheets were cold rolled at ambient temperature to various levels of reduction in thicknesses ranging from 5 to 25%.

2.3 Heat Treatment

Parvathavarthini and Dayal have established time-temperature-sensitization diagrams for this material.[19] From these diagrams, three heat treatments were selected in order to sensitize this stainless steel to different degrees of sensitization (DOS). When this material is exposed to 898 K for 10, 20, and 50 h, it becomes sensitized for all levels of cold work. Hence, the following heat treatments were carried out for all levels of cold work:

- 898 K-10 h-air cooling,
- 898 K-20 h-air cooling, and
- 898 K-50 h-air cooling.

Table 1 Chemical composition of AISI 316 SS

Element	Wt%
C	0.043
N	0.075
Cr	17.2
Ni	10.2
Mo	1.85
Mn	1.54
P	0.022
S	0.005
Si	0.585
V	0.061
Cu	0.207
Co	0.230
Fe	Balance

2.4 Specimen Preparation

From every cold-worked and heat-treated material, specimens of size 10 × 10 mm were cut for performing ASTM A262 practice A test and electrochemical potentiokinetic reactivation (EPR) test.[20] The balance specimen was used for treatment by laser beam. The specimens for ASTM A262 practice A test and EPR test were mounted in epoxy resin and were polished up to fine diamond (3 μm) finish. After polishing, the specimens were ultrasonically cleaned with soap solution and distilled water and finally were dried.

2.5 ASTM A262 Practice A Test

This test consists of electrolytically etching a polished specimen in 10 wt.% ammonium persulfate solution at room temperature at a current density of 1 A/cm^2 for 5 min. The etched structure was then examined at 200× using an optical microscope. Under these etching conditions, chromium carbide is dissolved preferentially and the microstructure gives an idea of chromium depletion, which is responsible for IGC. If there is no carbide precipitation, a "step" structure is obtained, because of the difference in the rate of etching of variously oriented grains. A "dual" structure is obtained if chromium carbide precipitation is discontinuous. A "ditch" structure is obtained if the grain boundaries are completely surrounded by chromium carbide. Even if one grain is completely surrounded by ditch, it is characterized as a ditch structure. All specimens were subjected to this test before and after LSM.

2.6 EPR Test

A single-loop EPR test was carried out for all the cold-worked and sensitized specimens as per the procedure described

in ASTM standard G108.[20] 0.5 M sulfuric acid containing 0.01 M ammonium thiocyanate was the medium in which the EPR tests were done. Dry, oxygen-free, argon gas was purged for a period of 0.5 h into the test solution, and gas purging was continued throughout the experiment. The specimen was immersed in the solution for 15 min before starting the polarization. The scan speed was 6 V/h and it was achieved with a potentioscan (model POS 73 Wenking). The specimen was kept at +200 mV (SCE) for 2 min. After passivation, the specimen was cathodically polarized to corrosion potential, and the current versus potential plots were recorded using an X-Y recorder. After the EPR measurements, every specimen was examined under optical microscope to ensure that the reactivation peak is due to alloy depletion and not due to localized attack such as pitting. Grain boundary grooving in the optical micrograph is an indication of IGA. The reproducibility of the single-loop EPR experiment was highly dependent upon the initial surface finish of the specimen. Even a minor variation in the surface finish produced considerable difference in the magnitude of the peak. By preparing the test solution just before use, so as to avoid the degradation of thiocyanate in sulfuric acid, by polishing the specimen before exposure, and by cathodically cleaning the specimen by keeping it at −500 mV (SCE) for 5 min before starting the scan, the reproducibility was greatly improved. The area under the reactivation peak was calculated, which gives the total quantity of electric charge passing through the surface, which is exposed, to the solution. From the reactivation charge, the reactivation charge density (Q) was calculated for all the specimens before LSM.

2.7 Laser Surface Melting

Each cold-worked and sensitized specimen was subjected to LSM using an indigenous 500 W multibeam cw CO_2 laser. Melting was attempted at various power levels, viz. 150, 200, 250, and 260 W, for different interaction times ranging from 5 to 30 s. Several combinations of power and interaction time were used to select an optimum value of energy. Very low energy may not be sufficient to homogenize sensitized microstructure by dissolving $M_{23}C_6$ carbides. On the contrary, use of a very high-energy beam may result in complete elimination of sensitized microstructure over the entire cross section of the specimen. These two constraints set the upper and lower limits within which a most suitable combination of power and interaction time needs to be chosen in such a way as not to miss the aim of the investigation, *viz.* identification of influence of cold work on the desensitization behavior of this stainless steel. Moreover, this choice is critical in restricting the melting of the superfluous top layers alone, without affecting the underlying microstructure. A laser power of 250 W and dwell time of 20 s satisfied all the above requirements as checked by micrography. In an actual situation, one does not need to melt the surface to attain homogenization of microstructures using laser treatment. The heat generated on the surface upon laser irradiation depends on several parameters, such as power density of the beam and its dwell time, absorptivity, specific conductivity of the substrate material, as well as the surface condition before the irradiation. To ensure that the adjacent layers are completely austenitized, in this study, the surface layers were allowed to melt. Hence, all the specimens were melted using these optimized parameters.

In addition, melting was also carried out using another commercial 9 kW cw CO_2 laser using laser power of 5 kW and traverse speed of 20 mm/s. Only mill-annealed and 25% cold-worked specimens were melted under these conditions.

2.8 Measurement of Width of Desensitized Zone

After laser melting, the cross sections of the specimens were polished and subjected to ASTM A262 practice A test. The laser-melted zone, heat-affected zone, and unaffected bulk were identified. The width of the homogenized (desensitized) zone was measured for all the specimens.

2.9 EPR Test after LSM

After locating the desensitized zone using the ASTM A262 practice A test as described in Section 2.8, the surface was repolished up to a fine diamond (3 μm) finish. Using 3M electroplating tape, the laser-melted zone and unaffected base metal were masked, leaving only the desensitized zone. The single-loop EPR experiment was done by exposing only the desensitized zone, as described in Section 2.6, and the reactivation charge density (Q) was calculated for all laser-melted specimens.

3. Results and Discussion

Aging the specimens at 898 K for 10, 20, and 50 h results in different DOS for all levels of cold work studied in this investigation. The choice of this sensitizing temperature and aging time enabled us to establish the influence of prior cold work and DOS on the extent of desensitization due to LSM under identical melting conditions.

3.1 Metallographic Analysis

Microstructure of Cold-Worked and Sensitized 316 SS. The microstructures obtained for all cold-worked specimens when aged at 898 K for 10, 20, and 50 h are presented in Fig. 1(a) to (f), Fig. 2(a) to (f), and Fig. 3(a) to (f). Because all the specimens are in the sensitized condition, a "ditch" structure was revealed for all the specimens. For as-received (0% CW) and 5% CW material, $M_{23}C_6$ precipitation takes place predominantly along the grain boundaries (Fig. 1a and b, Fig. 2a and b, and Fig. 3a and b). For 10 and 15% CW specimens, aging for 20 and 50 h leads to precipitation within the grains in addition to the grain boundaries (Fig. 1c and d, Fig. 2c and d, and Fig. 3c and d). For 20 and 25% CW specimens, all three aging treatments result in extensive intra- and intergranular precipitation.

Microstructure after Laser Melting. Figure 4(a) to (c) represent the scanning electron micrographs of the laser-melted specimen (898 K-50 h-25% CW). Three distinctly different regions were revealed by electrolytic etching. When melted using cw CO_2 laser at 5 kW with a traverse speed of 20 mm/s, the thickness of the melted zone was approximately 220 to 290 μm. Chromium carbides formed during the sensitization treatment are not stable above 1273 K. During LSM, a thin

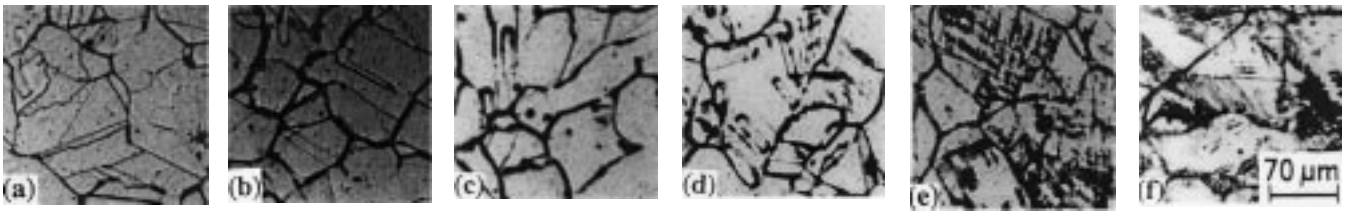

Fig. 1 (**a**) to (**f**) Microstructures obtained for AISI 316 SS sensitized at 898 K for 10 h: (**a**) 0% CW, (**b**) 5% CW, (**c**) 10% CW, (**d**) 15% CW, (**e**) 20% CW, and (**f**) 25% CW

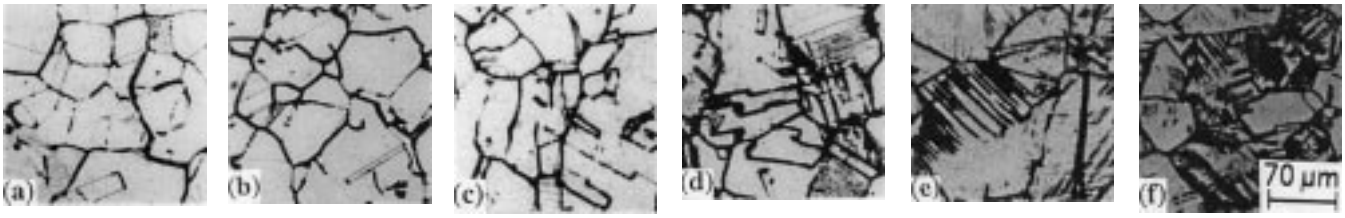

Fig. 2 (**a**) to (**f**) Microstructures obtained for AISI 316 SS sensitized at 898 K for 20 h: (**a**) 0% CW, (**b**) 5% CW, (**c**) 10% CW, (**d**) 15% CW, (**e**) 20% CW, and (**f**) 25% CW

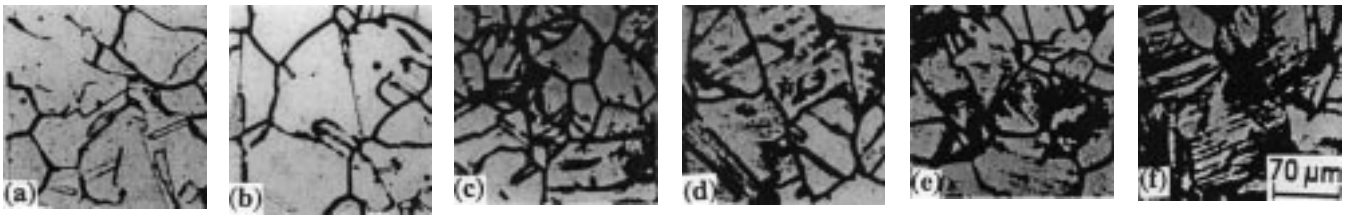

Fig. 3 (**a**) to (**f**) Microstructures obtained for AISI 316 SS sensitized at 898 K for 50 h: (**a**) 0% CW, (**b**) 5% CW, (**c**) 10% CW, (**d**) 15% CW, (**e**) 20% CW, and (**f**) 25% CW

surface layer reaches a temperature above the melting temperature of the alloy. Hence, all the carbides are expected to decompose in the melted pool. Further, the alloying elements in the melted pool including Cr and Mo are redistributed within the specimen, aided by (1) diffusion, which arises due to the concentration difference of chromium in chromium-rich $M_{23}C_6$ carbides and the matrix, and by (2) fluid flow/convection induced by the thermal gradient at the free surface of the melted pool.[7] Because of the rapid solidification, a dendritic cellular structure was obtained in the laser-melted zone, as shown in Fig. 4(a). During LSM, the region outside the fusion zone will experience a temperature in the range of $T_M \leq T \leq T_{RT}$ (T_M—melting temperature of the alloy, and T_{RT}—room temperature). Temperatures are high in the vicinity of the fusion line and decrease far from it. Depending upon the temperature profiles, cooling rate, and interaction time, continuous $M_{23}C_6$ carbides present in the sensitized specimen dissolve and the ditch structure gets eliminated. Alloying elements get redistributed, resulting in the nominal composition of 18%. Hence, this zone shows a "step" structure and is presented in Fig. 4(b). At the interface between heat-affected zone and unmelted zone, globular particles of $M_{23}C_6$ are discontinuously distributed. Because the alloy depletion around these particles is discontinuous, failure due to IGC or IGSCC is less likely. The unaffected base metal with original sensitized microstructure is shown in Fig. 4(c) along with the desensitized zone and discontinuous globular $M_{23}C_6$ precipitate.

All the laser-melted specimens were examined under an optical microscope in order to assess whether any systematic trend existed between the degree of prior cold work and the extent of desensitization due to LSM. For this purpose, the widths of the laser-melted zone and desensitized zone were measured at several locations for each specimen. Because the

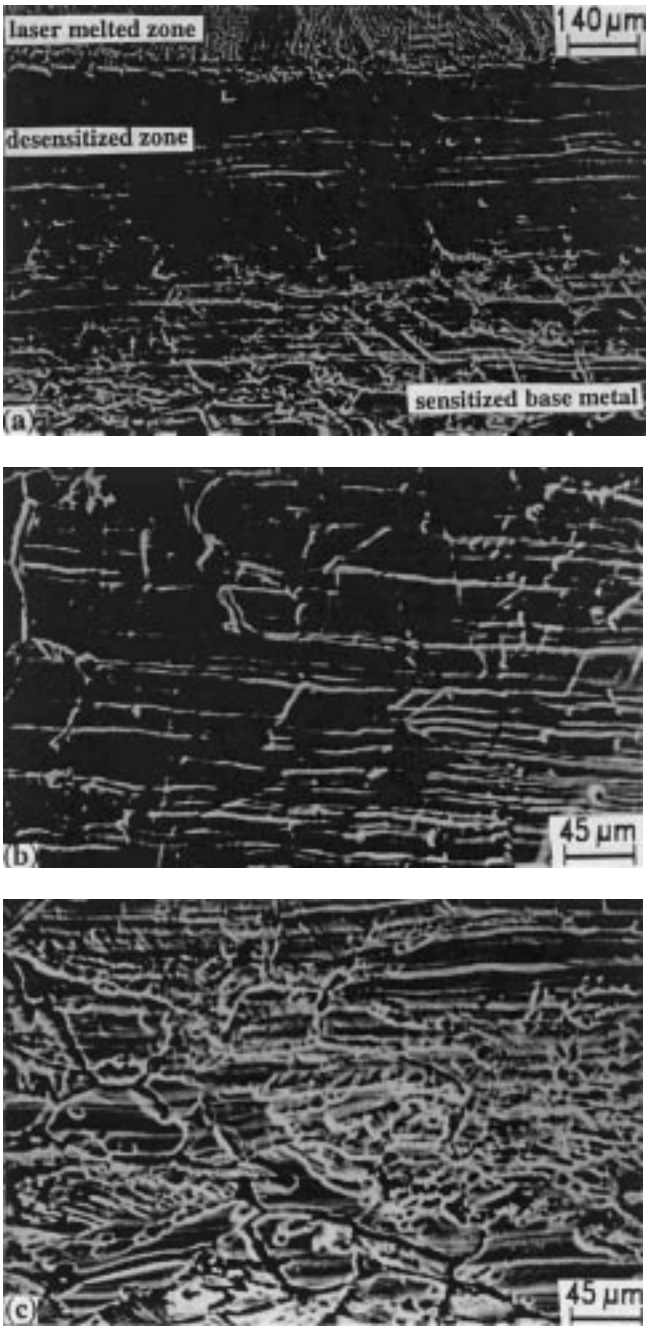

Fig. 4 (**a**) to (**c**) SEM of laser-melted AISI 316 SS (898 K-50 h-25% CW): (**a**) laser-melted zone, desensitized zone, and unaffected base metal; (**b**) desensitized zone showing step structure with globular carbides distributed discontinuously; and (**c**) desensitized zone/base metal interface showing disappearance of ditch structure and formation of globular carbides

variations in the width are quite significant, the average of several measurements is tabulated in Table 2(a) and (b). Analysis of the data indicates that, as the % CW increases, there is a systematic decrease in the width of the desensitized zone under identical laser melting conditions. Fig. 5(a) to (c) clearly show that the "desensitized structure" is quite a bit wider for the as-received material (0% CW) compared to the 25% cold-worked specimen, for which it is very narrow.

Table 2(a) Width of the desensitized zone after LSM (250 W-20 s)

	Width of the desensitized zone (μm)		
%CW	898 K/10 h	898 K/20 h	898 K/50 h
0	2708 ± 100	1769 ± 200	2440 ± 62
5	2074 ± 250	. . .	1037 ± 17
10	2257 ± 100	1098 ± 217	854 ± 27
15	1732 ± 215	732 ± 20	732 ± 70
20	1488 ± 75	671 ± 75	509 ± 18
25	1098 ± 18	549 ± 15	243 ± 16

Table 2(b) Width of the desensitized zone after LSM (5 kW-20 mm/s)

	Width of the desensitized zone (μm)		
%CW	898 K-10 h	898 K-20 h	898 K-50 h
0	2220 ± 10	2440 ± 20	1952 ± 11
25	500 ± 2	427 ± 23	390 ± 7

3.2 EPR Test

The reactivation charge densities (Q) obtained for all the specimens in the cold-worked and sensitized condition before and after LSM are collectively given in Table 3(a) to (d). It can be seen from these data that, as the aging time increases, the DOS increases due to the increase in the depletion in alloying elements, resulting in a higher Q value.

For every specimen, the Q value is lesser for the laser-melted specimen compared to the unmelted one. This point is illustrated in Fig. 6(a) to (f). For the sake of brevity, only the curves obtained for 0 and 25% CW specimens laser melted using cw CO_2 (5 kW-traverse speed: 20 mm/s) are presented. The peak potential (E_{peak}) at which the current density is maximum in the reactivation peak is significantly lower for LSM specimens compared to the corresponding unmelted specimen. Muraleedharan *et al.*[21] and Cowan and Tedmon[22] have attributed this difference in E_{peak} to the composition of the alloy and have reported that the one with higher Cr and Mo will have much lower E_{peak} values. Because in our studies LSM specimens show lower E_{peak} values compared to as-sensitized specimens, homogenization and redistribution of chromium and molybdenum can be clearly understood. The lower values of these two parameters prove that LSM has resulted in desensitization by dissolving the continuous network of $M_{23}C_6$ carbides and redistributing the alloying elements that are responsible for passivity.

In order to understand the influence of CW on the extent of homogenization in the desensitized zone, a homogenization index (H) was calculated from the Q values obtained before and after LSM as follows:

$$H = 1 - [Q_{LM}/Q_S]$$

where H is the homogenization index and Q_{LM} and Q_S are the

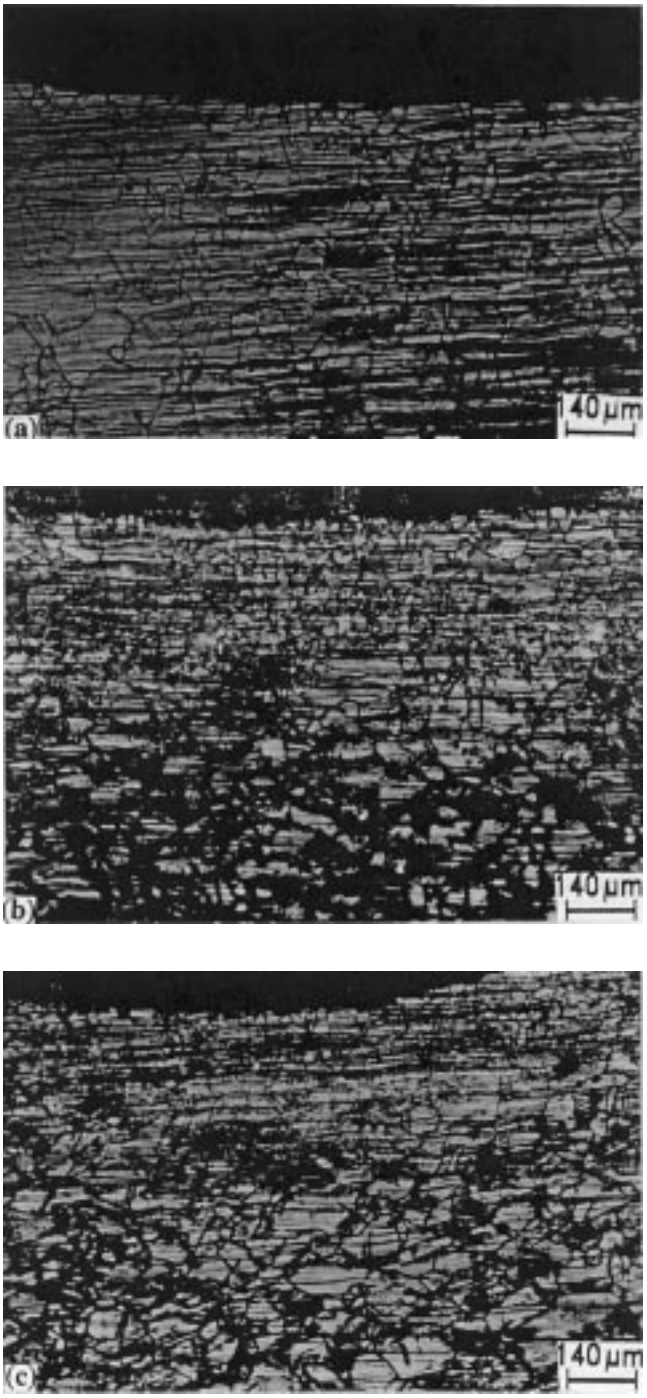

Fig. 5 (**a**) to (**c**) Microstructure of the cross section of AISI 316 SS sensitized at 898 K for 50 h after LSM (250 W/20 s): (**a**) 0% CW, (**b**) 20% CW, and (**c**) 25% CW

reactivation charge densities for laser-melted and sensitized specimens, respectively. Because LSM results in the elimination of the chromium-depleted zone and the homogenization of alloying elements required for passivity, the dissolution from the chromium-depleted zone is significantly less, resulting in lower Q values. Because Q_{LM}; becomes low due to homogenization, $1 - Q_{LM}/Q_S$ will be high and, hence, H can be taken as a direct measure of the extent of homogenization.

Table 3(a) Results obtained in EPR test for specimens, heat treated at 898 K for 10 h before and after LSM (250 W/20 s)

Heat treatment/%CW	Q (mC/cm^2)		Homogenization index
	Before LSM	After LSM	
898 K-10 h-0% CW	12.7	0.2	0.98
898 K-10 h-5% CW	14.4	0.3	0.98
898 K-10 h-10% CW	29.4	1.4	0.95
898 K-10 h-15% CW	34.1	…	…
898 K-10 h-20% CW	53.2	4.1	0.92
898 K-10 h-25% CW	70.6	11.7	0.83

Table 3(b) Results obtained in EPR test for specimens, heat treated at 898 K for 20 h before and after LSM (250 W/20 s)

Heat treatment/%CW	Q (mC/cm^2)		Homogenization index
	Before LSM	After LSM	
898 K-20 h-0% CW	61.4	1.1	0.98
898 K-20 h-5% CW	113.7	5.8	0.95
898 K-20 h-10% CW	151.7	2.1	0.99
898 K-20 h-15% CW	157.4	6.5	0.96
898 K-20 h-20% CW	286.4	8.0	0.96
898 K-20 h-25% CW	449.4	31.5	0.93

Table 3(c) Results obtained in EPR test for specimens heat treated at 898 K for 50h before and after LSM (250 W/20 s)

Heat treatment/%CW	Q (mC/cm^2)		Homogenization index
	Before LSM	After LSM	
898 K-50 h-0% CW	122.0	1.2	0.99
898 K-50 h-5% CW	160.6	6.6	0.96
898 K-50 h-10% CW	346.0	13.1	0.96
898 K-50 h-15% CW	444.7	14.0	0.97
898 K-50 h-20% CW	529.3	18.1	0.97
898 K-50 h-25% CW	667.8	46.2	0.93

Table 3(d) Results obtained in EPR test for 0% CW and 25% CW specimens before and after LSM (5 kW-20 mm/s)

Heat treatment/%CW	Q (mC/cm^2)		Homogenization index
	Before LSM	After LSM	
898 K-10 h-0% CW	12.7	No peak	1
898 K-10 h-25% CW	70.6	0.5	0.99
898 K-20 h-0% CW	61.4	1.8	0.97
898 K-20 h-25% CW	449.4	38.2	0.92
898 K-50 h-0% CW	122	2.9	0.98
898 K-50 h-25% CW	667.8	187.7	0.72

From Table 3(a) to (d), it is very clear that, for every sensitizing heat treatment, the extent of homogenization in the HAZ

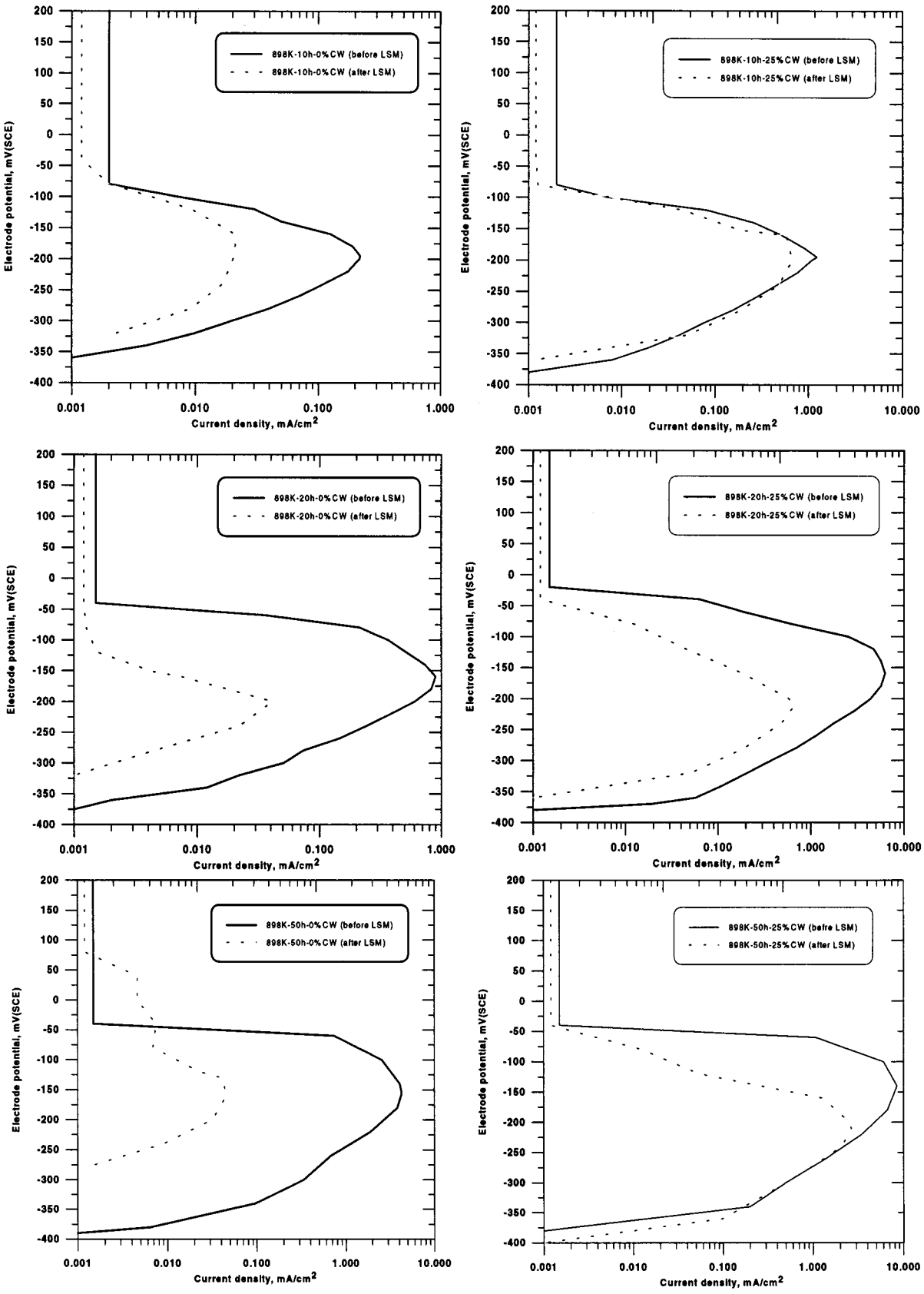

Fig. 6. EPR curves for cold-worked and sensitized 316 SS before and after LSM

is maximum for 0% CW and minimum for 25% CW under identical laser melting conditions.

The salient features of the investigation may be summarized briefly as follows.

- For each cold work, as the aging time at 898 K increases, the $M_{23}C_6$ precipitation and DOS increase
- For each sensitizing heat treatment, as the cold work level increases, the $M_{23}C_6$ carbide starts precipitating both along grain boundaries and the matrix.
- Under identical laser melting conditions, the width of the desensitized zone and the extent of homogenization decrease with the increase in cold work.

All these observations can be attributed to the structural changes taking place with the increasing degree of cold work and the effect of these changes on the chromium diffusion rate as well as nucleation and growth of carbides. With a small degree of cold work, a large increase in dislocation density in the grain boundary region is observed, which will help in the precipitation and growth of carbides at the grain boundary when heated in the sensitization range. The authors have reported that cold work leads to precipitation of finer carbides distributed at smaller intercarbide spacings, thus increasing the number of grain boundary carbides.[23] This will lead to a correspondingly large number of chromium-depleted zones. Apart from increasing the total area of the attacked region of the grain boundary, a decrease in intercarbide spacing would also enhance sensitization kinetics. 316 SS has a low stacking fault energy and, hence, a higher degree of cold work, resulting in a larger dislocation pileup on the slip planes than cellular dislocations. Due to this, slip planes become favorable sites for carbide precipitation. Therefore, as the degree of cold work increases, the extent of $M_{23}C_6$ carbide precipitation and, hence, (Mo + Cr) depletion also increases, resulting in higher E_{peak} and Q values. Because desensitization of cold-worked and sensitized microstructures by laser melting involves the relief of residual stresses and homogenization of the sensitized microstructure, by dissolving the continuous $M_{23}C_6$ network, and redistribution of alloying elements, a laser beam of higher energy or more interaction time must be adopted in the cold-worked structure to produce the same extent of homogenization as that of the mill-annealed (as-received) material.

4. Summary and Conclusions

The possibility of improving IGC and IGSCC resistance of cold-worked and sensitized steel was investigated by melting the surface of nitrogen containing 316 SS using cw CO_2 laser at (1) 250 W/20 s and (2) 5 kW, with a traverse speed of 20 mm/s. Optical metallography, scanning electron microscopy, and ASTM standards A262 and G108 were followed to characterize the laser-melted and heat-affected zones. The width of the desensitized zone and the extent of homogenization in the desensitized zone systematically decrease with the increase in CW. It was proved that elimination of the complex microstructure arising due to CW and sensitization could be effected without affecting the bulk properties by LSM at appropriate conditions. Because the sensitized microstructure is homogenized and residual stresses due to cold work are relieved, IGSCC resistance of the laser surface melted material is improved. The salient feature of the investigation is that, if a component that has undergone cold working during fabrication gets sensitized, laser melting/heating at higher power levels and an extended interaction time must be resorted to in order to achieve homogenization comparable to a sensitized material, which has not undergone prior deformation.

Acknowledgments

The authors acknowledge the support of Dr. Baldev Raj, Director of the Materials, Chemistry and Reprocessing Group, and Dr. V.S. Raghunathan, Associate Director, Materials Characterisation Group, Kalpakkam, during the course of this investigation. The authors thank Smt. K. Parimala for her assistance in the metallography and electrochemical experiments.

References

1. Durgam G. Chakrapani: in *Hand Book of Case Histories of Failure Analysis*, Kholefa A. Esakul, ed., ASM International, Materials Park, OH, 1992, pp. 164-67.
2. Durgam G. Chakrapani: in *Hand Book of Case Histories of Failure Analysis*, Kholefa A. Esakul, ed., ASM International, Materials Park, OH, 1992, pp. 168-70.
3. Harry E. Ebert: in *Hand Book of Case Histories of Failure Analysis*, Kholefa A. Esakul, ed., ASM International, Materials Park, OH, 1992, pp 278-83.
4. F. Karahira, K. Hirano, Y. Tanaka, K. Yoshida, M. Kuribayashi, and T. Umemmoto: *Nucl. Eng. Design*, 1994, vol. 153, p. 111.
5. U. Kamachi Mudali, R.K. Dayal, and G.L. Goswami: *Surface Eng.*, 1995, vol. 11, p. 1.
6. J. Stewart, D.B. Wells, P.M. Scott, and A.S. Bransden: *Corrosion*, 1990, vol. 46, p. 618.
7. O.V. Akgun and O.T. Inal: *J. Mater. Sci.*, 1992, vol. 27, p. 2147.
8. M. Koso and H. Miyuki: *Sumitomo Met.*, 1989, vol. 1, p. 47.
9. I. Masumoto, T. Shinoda, and T. Hirate: *Q. J. Jpn. Welding Soc.*, 1989, vol. 7, p. 73.
10. J. de Damborena, A.J. Vazquez, J.A. Gonzalez, and D.R.F. West: *Surface Eng.*, 1989, vol. 5, p. 235.
11. A. La Barbera, S. Martelli, and A. Mignone: *Laser Treatment of Materials*, DGM InformationsgesellschaftmbH, Oberursel, 1987, p. 79.
12. S.V. Deshmukh, C. Rajagopalan, R.V. Subba Rao, R.K. Dayal, and J.B. Gnanamoorthy: *Proc. National Laser Symp.*, Dehradun, Department of Atomic Energy, India, 1995, p. 312.
13. Y. Nakao and K. Nishimoto: *J. Jpn. Welding Soc.*, 1987, vol. 5, p. 15.
14. C.H. Lee, K.C. Kim, and R.W. Chang: *Kor. Inst Mater.*, 1992, vol. 30, p. 43.
15. U.K. Mudali and R.K. Dayal: *J. Mater. Eng. Performance*, 1992, vol. 1, p. 341.
16. U.K. Mudali, R.K. Dayal, J.B. Gnanamoorthy, S.M. Kanetkar, and S.B. Ogale: *Metall. Trans. JIM*, 1991, vol. 32, p. 845.
17. J.Y. Jeng, B.E. Quayle, P.J. Modem, W.M. Steen, and B.D. Bastow: *Corr. Sci.*, 1993, vol. 35, p. 1289.
18. S. Zamfir and R. Vidu: *Processes & Materials Innovation Stainless Steel*, Associazione Italiana di Metallurgia, Milano, Italy, 1993, vol. 3, p. 3.161.
19. N. Parvathavarthini and R.K. Dayal: Indira Gandhi Centre for Atomic Research, Kalpakkam, Tamilnadu, India, unpublished.
20. *Annual Book of ASTM Standards*, ASTM, Philadelphia, PA, 1990, vol. 03.02.

21. P. Muraleedharan, J.B. Gnanamoorthy, and K. Prasad Rao: *Corrosion*, 1989, vol. 45, p. 142.
22. R.L. Cowan and C.S. Tedmon: *Advances in Corrosion Science and Technology*, Plenum Press, New York, NY, 1973, vol. 3, p. 293.
23. S.K. Mannan, R.K. Dayal, M. Vijayalakshmi, and N. Parvathavarthini: *J. Nucl. Mater.*, 1984, vol. 126, p. 1.